

# Three-step approach for computing band offsets and its application to inorganic $ABX_3$ halide perovskites

Li Lang,<sup>1</sup> Yue-Yu Zhang,<sup>1</sup> Peng Xu,<sup>1</sup> Shiyu Chen,<sup>2</sup> H. J. Xiang,<sup>1,3,\*</sup> and X. G. Gong<sup>1,3,†</sup>

<sup>1</sup>Key Laboratory for Computational Physical Sciences (Ministry of Education), State Key Laboratory of Surface Physics, and Department of Physics, Fudan University, Shanghai 200433, China

<sup>2</sup>Laboratory of Polar Materials and Devices, East China Normal University, Shanghai 200241, China

<sup>3</sup>Collaborative Innovation Center of Advanced Microstructures, Nanjing 210093, Jiangsu, People's Republic of China

(Received 17 March 2015; revised manuscript received 22 May 2015; published 3 August 2015)

Band offsets between different semiconductors are important parameters that determine the electronic transport properties near the interface in the heterostructure devices. The computation of the natural band offset is a well-known challenge. In this paper, we propose a new method, which is called the three-step method, to accurately predict the natural band offset. Compared to previous methods, the present method is more direct and can be easily applied to systems with larger lattice mismatch and to systems with lower symmetry. Using the present method, we successfully calculate the natural band offset between the inorganic halide perovskites  $ABX_3$  ( $A = \text{Cs}$ ;  $B = \text{Sn, Pb}$ ;  $X = \text{Cl, Br, I}$ ) in the cubic and orthorhombic phase. We show that the valence band maximum shifts down as the atomic number of the  $X$  site ion increases, while the valence band maximum shifts up as  $B$  site ion varies from Sn to Pb or as the compound transforms from the cubic phase to the orthorhombic phase. It is found that the band gap differences between these compounds can be attributed primarily to the valence band offsets, with a much smaller contribution from the conduction band offsets.

DOI: 10.1103/PhysRevB.92.075102

PACS number(s): 61.50.Ah, 71.20.Nr, 71.55.Ht, 72.40.+w

## I. INTRODUCTION

I-IV-VII<sub>3</sub> materials with halide perovskite structures (denoted as  $ABX_3$ , such as  $\text{CsSnI}_3$  and  $\text{CH}_3\text{NH}_3\text{PbI}_3$ ) have shown a great potential to be good solar-cell materials and have drawn great interest [1–22]. Based on  $\text{CH}_3\text{NH}_3\text{PbI}_3$ , Zhou *et al.* have achieved a power conversion efficiency of 19.3%, which is comparable to those of today's best thin-film photovoltaic devices [8]. To improve the performance of these compounds, their properties, such as stability, resistivity, light-absorption spectra, and carrier mobility, have been studied experimentally [8–10].

Besides the intrinsic nature of the material, the interface property is of great importance to the efficiency of the photovoltaic devices. The natural band offset between different compounds is a vital parameter in the interface design because it determines the transport properties and charge transfer between different compounds in the device. Unfortunately, accurate band alignments between  $ABX_3$ -type halide perovskite photovoltaic materials are currently not available, because the computation of natural band offset is a nontrivial problem due to uncertainty of the energy reference in the infinite system and low symmetry where the previously proposed method based on absolute deformation potential (ADP) cannot be easily applied. In this paper, we develop a simple, general, direct approach, i.e., a three-step approach, for computing the band offsets that can be applied to a variety of materials. With this new approach, we can calculate the band offsets between  $ABX_3$ -type halide perovskites systematically. These results are expected to provide a new guideline on optimizing the performance of  $ABX_3$ -based solar cell devices. In the rest of the paper, we first discuss the three-step method in detail

and then present our calculated results and discuss the general chemical trends of the obtained results.

## II. THREE-STEP METHODS

In a pioneering paper, Wei and Zunger [23] followed the procedure in photoemission core-level spectroscopy [24] and constructed a superlattice to calculate the valence band offset  $\Delta E_v(L/R)$  between two hypothetical compounds  $L$  and  $R$ , where the valence band offset is defined as

$$\Delta E_v(L/R) = \Delta E_{v,C^*}^R - \Delta E_{v,C}^L + \Delta E_{C,C^*}^{L/R}. \quad (1)$$

Here,

$$\Delta E_{v,C}^L = E_v^L - E_C^L \quad (2)$$

is the energy difference between the core level and the valence band maximum (VBM) for pure  $L$  (and similar for  $R$ ), and

$$\Delta E_{C,C^*}^{L/R} = E_{C^*}^R - E_C^L \quad (3)$$

is the energy difference in the core levels ( $C$  and  $C^*$ ) between  $L$  and  $R$  on each side of the interface, which can be obtained from the calculation of an  $L_n/R_n$  (001) heterojunction supercell. Here, core levels of  $L$  and  $R$  in the bulk are assumed to be the same as that in the supercell, ignoring the influence from the volume deformation to the core level, so this method is suitable only for systems with negligible lattice mismatch [25–27]. In order to take this effect into account, Li *et al.* developed an ADP correction method [28–30]. They first calculated the band offsets between the two compounds with the averaged lattice constant using an expression similar to Eq. (1):

$$\Delta E_v^{(av)}(L/R) = \Delta E_{v,C^*}^{(av)}(R) - \Delta E_{v,C}^{(av)}(L) + \Delta E_{C,C^*}^{(av)}(L/R) \quad (4)$$

Then the VBM absolute volume-deformation potential  $\alpha_{\text{VBM}}$  of  $L$  and  $R$  was computed through the procedure

\*Corresponding author: hxjiang@fudan.edu.cn

†Corresponding author: xggong@fudan.edu.cn

proposed by Li *et al.* [28,29]. After  $\Delta E_v^{(av)}(L/R)$  and  $a_{\text{VBM}}$  are obtained, the VBM states are corrected by  $a_{\text{VBM}} \frac{\Delta V}{V}$ , a linear term with volume changes, from the averaged lattice constant to the equilibrium lattice constant for both  $L$  and  $R$  to get the final natural band offset. The calculation of the VBM absolute volume-deformation potential is complex and is practically applicable only to high-symmetry systems. This method was proved to be accurate for high-symmetry systems with a small lattice mismatch since the correction is only up to linear approximation. For a low-symmetry and large lattice mismatch system, e.g., orthorhombic  $ABX_3$ -type compounds, the ADP correction method becomes unfeasible. To solve this problem, we developed a three-step method to predict the “natural” valence band offset.

Similar to the method developed by Wei and Zunger [23], we also construct superlattices made by the two compounds  $L$  and  $R$ . For simplicity, let's consider the case where the lattice vectors are mutually orthogonal to each other. The three-step approach can be generally applied to other systems. For the two compounds  $L$  and  $R$  with a lattice constant of  $(a_1, a_2, a_3)$  and  $(b_1, b_2, b_3)$ , respectively,  $\alpha = \beta = \gamma = 90^\circ$ , the valence band offset is defined as follows:

$$\Delta E_v(L/R) = \Delta E_{v,C^*}^R - \Delta E_{v,C}^L + \Delta E_{C,C^*}^{L/R} \quad (5)$$

Here,

$$\Delta E_{v,C}^L = E_v^L - E_C^L \quad (6)$$

is the core level to VBM energy separations for pure  $L$  (and similar for  $R$ ). The procedure to calculate the core level difference  $\Delta E_{C,C^*}^{L/R}$  between these two compounds can be decomposed into three steps, as illustrated in Fig. 1. In the first

step, we expand  $L$  along (100) by  $\frac{b_1-a_1}{a_1}$  (if the value is negative,  $L$  will be compressed); the expanded compounds can be noted as  $L'$  with a lattice constant of  $(b_1, a_2, a_3)$ . The core level difference  $\Delta E_{C,C'}^{L/L'}$  between  $L$  and  $L'$  can be obtained from the calculation for the  $L/L'$  superlattices with a (100) orientation. The second step is similar to the first step; we expand  $L'$  along (010) by  $\frac{b_2-a_2}{a_2}$  and get  $L''$  with a lattice constant of  $(b_1, b_2, a_3)$ . The core level difference  $\Delta E_{C',C''}^{L'/L''}$  between  $L'$  and  $L''$  can be obtained from the calculation for the  $L'/L''$  superlattices with a (010) orientation. At last, the core level difference  $\Delta E_{C'',C^*}^{L''/R}$  between  $L''$  and  $R$  can be obtained from the calculation for the  $L''/R$  superlattices with a (001) orientation. Then,  $\Delta E_{C,C^*}^{L/R}$  in Eq. (5) can be written as follows:

$$\Delta E_{C,C^*}^{L/R} = \Delta E_{C,C'}^{L/L'} + \Delta E_{C',C''}^{L'/L''} + \Delta E_{C'',C^*}^{L''/R} \quad (7)$$

The final formula to calculate the valence band offset  $\Delta E_v(L/R)$  between two compounds  $L$  and  $R$  can be written as follows:

$$\begin{aligned} \Delta E_v(L/R) = & \Delta E_{v,C^*}^R - \Delta E_{v,C}^L + \Delta E_{C,C'}^{L/L'} + \Delta E_{C',C''}^{L'/L''} \\ & + \Delta E_{C'',C^*}^{L''/R} \end{aligned} \quad (8)$$

Actually,  $L'$  and  $L''$  act as two bridge compounds here. We can also choose  $R'$  with a lattice constant of  $(a_1, b_2, b_3)$  and  $R''$  with a lattice constant of  $(a_1, a_2, b_3)$  as the bridge compounds and calculate the core level difference with the same procedure. We can even choose four bridge compounds, expanded  $L$  with a lattice constant of  $(\frac{a_1+b_1}{2}, a_2, a_3)$  and  $(\frac{a_1+b_1}{2}, \frac{a_2+b_2}{2}, a_3)$ , and compressed  $R$  with a lattice constant of  $(\frac{a_1+b_1}{2}, \frac{a_2+b_2}{2}, b_3)$  and

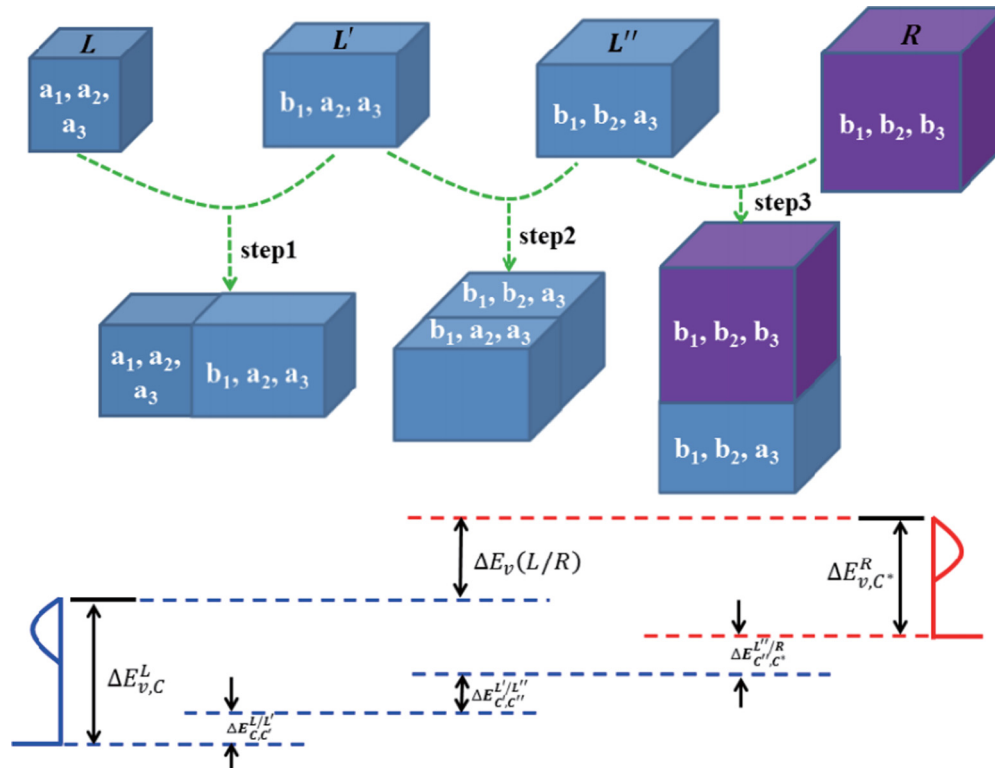


FIG. 1. (Color online) The schematic illustration of the three-step method for calculating the natural band offset.

$(\frac{a_1+b_1}{2}, b_2, b_3)$  and calculate the core level difference with five steps similar to the three-step method. According to our tests, all these methods give similar results. To obtain the conduction band offsets  $\Delta E_c$ , we use the relationship

$$\Delta E_c = \Delta E_g + \Delta E_v \quad (9)$$

where  $\Delta E_g$  is the measured band gap difference between  $L$  and  $R$ .

All of the preceding methods for computing band offsets use the core levels as the energy reference. However, one could also use the electrostatic potential as the energy reference [17,31–35]. These two energy references should give equivalent results. No matter which energy reference is chosen, the key problem is to calculate the energy difference between the energy reference in  $L$  and that in  $R$ . In the following, we use core levels as the energy reference to calculate the band offsets.

### III. COMPUTATIONAL DETAILS

Our calculations of  $ABX_3$  band offsets are performed using the density functional theory (DFT) as implemented in the plane wave Vienna *Ab Initio* Simulation Package (VASP) [36] code. For the exchange-correlation functional, the generalized gradient approximation (GGA) of Perdew-Burke-Ernzerhof (PBE) [37] is used. The projector-augmented wave (PAW) pseudopotentials [38] are used with an energy cutoff of 500 eV for the plane wave basis functions. Because PBE underestimates band gaps, we also use the  $GW^0$  method [39] to recalculate the band structures. Large numbers of k-point samples for Brillouin zone integration are used to ensure the convergence of the calculated results. The lattice vectors and atomic positions of each primitive cell are optimized according to the guidance of atomic forces, with a criterion that requires the calculated force on each atom smaller than 0.01 eV/Å. The spin-orbit coupling (SOC) effect is demonstrated to be strong in  $ABX_3$ -type compounds [15–17], so it's included in the calculations. In the band offset calculations, we take the 1s core levels of A, B, and X site atoms as a reference state, which are weighted as 1:1:3. The results calculated using different reference states are close.

### IV. RESULTS AND DISCUSSION

We first discuss the advantages of the three-step method by performing some test calculations. First, we apply the three-step method to calculate the band offsets of Si/Ge and GaAs/InAs; the valence band offsets of these two systems are 0.68 and 0.41 eV, respectively, which are close to the results predicted by the ADP correction method of 0.72 and 0.37 eV, respectively. Meanwhile, the results calculated with the traditional method (the method developed by Wei and Zunger [23]) are 0.86 and 0.08 eV, respectively. The experimental valence band offsets of Si/Ge and GaAs/InAs are about 0.70 eV [40,41] and 0.46 eV [42], respectively. These indicate that the results obtained with the three-step method and the ADP correction method are more accurate than those obtained with the traditional method and agree well with the experimental results. The traditional method assumes that the core level will not change with the lattice constant, so this method is only suitable for systems with negligible

TABLE I. Calculated band offsets (in electronvolts) between AlAs and GaAs using different methods. Deformation is applied for expanding AlAs and compressing GaAs. As the lattice mismatch (deformation) increases, the difference of the band offsets from the two methods increases.

Method	Deformation ratio					
	0	1%	2%	3%	4%	5%
ADP correction	0.49	0.39	0.30	0.21	0.14	0.07
Three-step	0.49	0.35	0.22	0.09	-0.03	-0.16
Difference	0.00	0.04	0.08	0.12	0.17	0.23

lattice mismatch and small ADP. The ADP correction method includes the core level changes during the volume deformation. Since this method assumes the ADP is a constant, it's a linear approximation. When the volume deformation becomes larger, linear approximation may become too crude. In this situation, the three-step method can still be used since no such approximation is made. To demonstrate this point, we take AlAs and GaAs as an example. They have no lattice mismatch at the equilibrium lattice, and both methods give the same band offset of 0.49 eV, in agreement with the experimental results of 0.4 ~ 0.55 eV [43,44]. However, when we calculate the band offsets between the expanded AlAs and the compressed GaAs, as can be seen in Table I, the difference between the three-step method and the ADP correction method increases as the lattice mismatch increases, since the error of the ADP correction method becomes larger. In addition, using the exactly solvable three-dimensional infinite square potential well model, we demonstrate that the three-step method is an exact method. The error of the ADP correction method is much less than the error of the traditional method, and the ratio of these two errors is approximately equal to the lattice mismatch ratio.

Now we calculate the band alignment between  $ABX_3$ -type compounds with different phases using the three-step method.  $ABX_3$ -type compounds show various phases at different temperatures [13,14], but the cubic structure [ $\alpha$  phase, Fig. 2(a)] is a typical high temperature phase and the orthorhombic structure [ $\gamma$  phase, Fig. 2(b)] is a typical low temperature phase, so we focus on these two phases in this paper. First, we calculate the valence band offset among CsSnCl<sub>3</sub>, CsSnBr<sub>3</sub>, CsSnI<sub>3</sub>, CsPbCl<sub>3</sub>, CsPbBr<sub>3</sub>, and CsPbI<sub>3</sub> in the cubic phase using Eq. (8). Then, we calculate the valence band offset between the cubic and the orthorhombic phases for each compound. Once the position of the VBM is obtained, the position of the conduction band maximum (CBM) can also be predicted using Eq. (9). Since PBE and even Heyd-Scuseria-Ernzerhof (HSE) underestimates the band gaps of this system [15,16], we perform the  $GW^0$  calculation to correct the band edges of each compound and thus obtain the accurate band alignments.

Band alignment results of the cubic compounds calculated using the PBE functional and  $GW^0$  correction are plotted in Fig. 3(a). It's clear that  $GW^0$  correction induces a large downshift of the VBM and relatively smaller upshift of the CBM. Figure 3(b) shows the corrected band edges of both cubic and orthorhombic compounds. The band gaps of

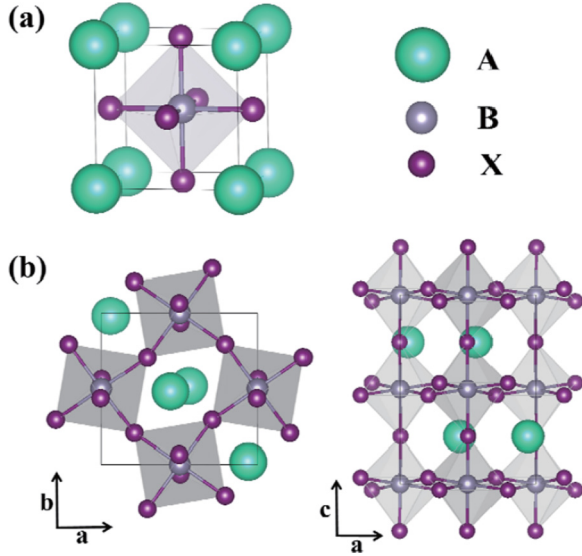


FIG. 2. (Color online) Perspective views of the (a) cubic and (b) orthorhombic phases of  $ABX_3$  halide perovskite.

$\alpha$ -CsPbCl<sub>3</sub>,  $\alpha$ -CsPbBr<sub>3</sub>, and  $\gamma$ -CsSnI<sub>3</sub> calculated using GW<sup>0</sup> approach are 3.03, 2.30, and 1.34 eV, respectively, in good agreement with the experimental results of 3.0, 2.3, and 1.3 eV, respectively [2,45]. We also calculated the band alignment between cubic  $ABX_3$  compounds using the ADP correction

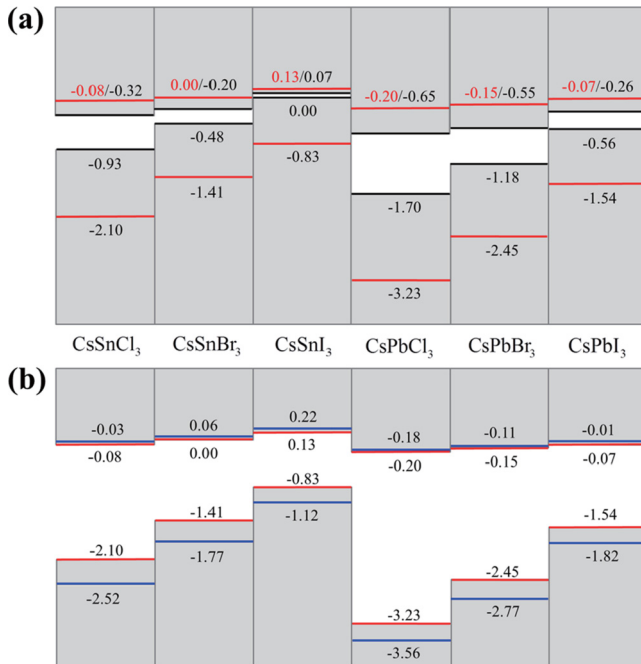


FIG. 3. (Color online) Calculated natural band alignment for the VBM and CBM of CsSnCl<sub>3</sub>, CsSnBr<sub>3</sub>, CsSnI<sub>3</sub>, CsPbCl<sub>3</sub>, CsPbBr<sub>3</sub>, and CsPbI<sub>3</sub> (a) in the cubic phase using the PBE functional (black lines) and GW<sup>0</sup> approach (red lines) and (b) in the cubic (red lines) and orthorhombic (blue lines) phases using the GW<sup>0</sup> approach. The VBM of cubic CsSnI<sub>3</sub> calculated using the PBE functional is set to zero as the reference. The effects of SOC are included in both situations.

method, and the results are similar to the three-step method, since here lattice mismatch for the cubic phase is small. In the following, we analyze the chemical trends of the band edges in detail based on the GW<sup>0</sup> corrected results.

As the  $B$  site ion varies from Sn to Pb, both VBM and CBM downshift. However, the downshift of VBM is much larger than that of CBM, so the band gap becomes larger. According to our calculation [15], the VBM of  $ABX_3$  is mainly the antibonding component of the hybridization between  $B$   $s$  states and  $Xp$  states, while the CBM is almost a nonbonding state dominated by the  $Xp$  orbitals. Since Sn  $5s$  orbital energy is higher than that of Pb  $6s$  and closer to the  $Xp$  energy levels, the  $s$ - $p$  hybridization is stronger between Sn  $s$ - $Xp$  than between Pb  $s$ - $Xp$ . The stronger coupling between Sn  $s$  and  $Xp$  upshifts the VBM, resulting in a higher VBM level than that in the Pb case. Since the Sn  $5p$  state is 0.2 eV higher than that of Pb  $6p$ , the CBM level in the Sn-based compound is higher, by  $\sim 0.2$  eV, than that in the Pb case due to the nonbonding nature of the CBM.

As the  $X$  site ion changes from Cl to Br to I, both VBM and CBM upshift. However, the upshift of VBM is much larger than that of CBM, so the band gap decreases. VBM contains some  $p$  states of the  $X$  ion, and the energy level of  $Xp$  states increases from Cl to Br to I. Thus, the VBM becomes higher with  $X$  changes from Cl to Br to I; e.g., the  $Xp$  states orbital level increase is 0.89 and 1.20 eV with  $X$  changes from Cl to Br and from Br to I, respectively. But the VBM difference is reduced by  $s$ - $p$  hybridization; because the bond length is  $B$ -Cl <  $B$ -Br <  $B$ -I, hybridization becomes weaker and the antibonding VBM level shifts down when  $X$  ranges from Cl to Br to I. As a result, the valence band offset between  $\alpha$ -CsPbCl<sub>3</sub> and  $\alpha$ -CsPbBr<sub>3</sub> is reduced to 0.78 eV, and the valence band offset between  $\alpha$ -CsPbBr<sub>3</sub> and  $\alpha$ -CsPbI<sub>3</sub> is reduced to 0.91 eV (and similar for Sn-based compounds and compounds in the  $\gamma$  phase). The lattice constant becomes larger when  $X$  changes from Cl to Br to I. As a result, the Madelung potential becomes less attractive for electrons, which induces an upshift of the nonbonding CBM state. Butler *et al.* reported the band offsets between CH<sub>3</sub>NH<sub>3</sub>PbCl<sub>3</sub>, CH<sub>3</sub>NH<sub>3</sub>PbBr<sub>3</sub>, and CH<sub>3</sub>NH<sub>3</sub>PbI<sub>3</sub> and found a chemical trend similar to our results [46].

As shown in Fig. 2, each  $B$  ion has six neighboring  $X$  ions. When  $ABX_3$  transfers from the high temperature cubic phase to the low temperature orthorhombic phase, the  $B$ - $X$  bond length will no longer be the same as that in the cubic phase and will become three different, larger values as shown in Table II. Since the  $B$ - $X$  bond length becomes longer with

TABLE II. Calculated  $B$ - $X$  bond length (in angstroms) of  $ABX_3$  compounds (with  $A = \text{Cs}$ ;  $B = \text{Sn, Pb}$ ;  $X = \text{Cl, Br, I}$ ) in the cubic and orthorhombic phases.

Compound	Cubic		Orthorhombic	
	1	2	3	4
CsSnCl <sub>3</sub>	2.805	2.843	2.850	2.854
CsPbCl <sub>3</sub>	2.865	2.900	2.908	2.911
CsSnBr <sub>3</sub>	2.944	2.971	2.979	2.984
CsPbBr <sub>3</sub>	2.996	3.037	3.046	3.051
CsSnI <sub>3</sub>	3.140	3.178	3.188	3.193
CsPbI <sub>3</sub>	3.196	3.239	3.253	3.262

the phase transition, the hybridization becomes weaker and the antibonding VBM state shifts down with the phase transition. Meanwhile, the CBM will upshift a little due to the larger Madelung energy in the orthorhombic phase.

## V. CONCLUSIONS

We have developed a three-step method to accurately predict the “natural” band offset between compounds with different structures. This method is more accurate and general than the traditional method and the ADP correction method. Using this method, the band offsets between cubic and orthorhombic  $ABX_3$ -type compounds are predicted with  $\text{GW}^0$  corrected band gaps. The band gaps we calculated agree well with the available experimental results. The band gap differences between compounds with different  $B$  site ions, different

$X$  site ions, or different structures are attributed primarily to the valence band offset, with a much smaller contribution from the conduction band offset. This is essentially determined by the band character of the VBM and the CBM. Based on these results, we predict that the band gap of  $ABX_3$  can be tuned by atom substitution or phase transformation, which mainly changes the position of the VBM and can tune the conductivity of  $ABX_3$  in halide perovskite photovoltaic devices.

## ACKNOWLEDGMENTS

We are grateful for the discussion with Su-Huai Wei. This work was partially supported by the Special Funds for Major State Basic Research, National Natural Science Foundation of China (NSFC), Program for Professor of Special Appointment (Eastern Scholar). Computation was performed in the Supercomputer Center of Fudan University.

- 
- [1] A. Kojima, K. Teshima, Y. Shirai, and T. Miyasaka, *J. Am. Chem. Soc.* **131**, 6050 (2009).
- [2] I. Chung, B. Lee, J. He, R. P. H. Chang, and G. Kanatzidis, *Nature* **485**, 486 (2012).
- [3] M. M. Lee, J. Teuscher, T. Miyasaka, T. N. Murakami, and H. J. Snaith, *Science* **338**, 643 (2012).
- [4] L. Etgar, P. Gao, Z. Xue, Q. Peng, A. K. Chandiran, B. Liu, M. K. Nazeeruddin, and M. Gratzel, *J. Am. Chem. Soc.* **134**, 17396 (2012).
- [5] J. H. Noh, S. H. Im, J. H. Heo, T. N. Mandal, and S. I. Seok, *Nano Lett.* **13**, 1764 (2013).
- [6] A. Abrusci, S. D. Stranks, P. Docampo, H.-L. Yip, A. K.-Y. Jen, and H. J. Snaith, *Nano Lett.* **13**, 3124 (2013).
- [7] J. Burschka, N. Pellet, S. J. Moon, R. Humphry-Baker, P. Gao, M. K. Nazeeruddin, and M. Gratzel, *Nature* **499**, 316 (2013).
- [8] H. Zhou, Q. Chen, G. Li, S. Luo, T.-B. Song, H.-S. Duan, Z. Hong, J. You, Y. Liu, and Y. Yang, *Science* **345**, 542 (2014).
- [9] H.-S. Kim, C.-R. Lee, J.-H. Im, K.-B. Lee, T. Moehl, A. Marchioro, S.-J. Moon, R. Humphry-Baker, J.-H. Yum, J. E. Moser, M. Grätzel, and N.-G. Park, *Sci. Rep.-UK* **2**, 591 (2012).
- [10] C. C. Stoumpos, C. D. Malliakas, and M. G. Kanatzidis, *Inorg. Chem.* **52**, 9019 (2013).
- [11] J. H. Rhee, C. C. Chung, and E. W.-G. Diau, *NPG Asia Mater.* **5**, e68 (2013).
- [12] A. Poglitsch and D. Weber, *J. Chem. Phys.* **87**, 6373 (1987).
- [13] K. Yamada, S. Fuanbiki, H. Horimoto, T. Matsui, T. Okuda, and S. Ichiba, *Chem. Lett.* **20**, 801 (1991).
- [14] K. Yamada, Y. Kuranaga, K. Ueda, S. Goto, T. Okuda, and Y. Furukawa, *Bull. Chem. Soc. Jpn.* **71**, 127 (1998).
- [15] L. Lang, J.-H. Yang, H.-R. Liu, H. J. Xiang, and X. G. Gong, *Phys. Lett. A* **378**, 290 (2014).
- [16] L.-Y. Huang and W. R. L. Lambrecht, *Phys. Rev. B* **88**, 165203 (2013).
- [17] J. Even, L. Pedesseau, J. M. Jancu, and C. Katan, *J. Phys. Chem. Lett.* **4**, 2999 (2013).
- [18] I. Borriello, G. Cantele, and D. Ninno, *Phys. Rev. B* **77**, 235214 (2008).
- [19] Y. H. Chang, C. H. Park, and K. Matsuishi, *J. Korean Phys. Soc.* **44**, 889 (2004).
- [20] W.-J. Yin, T. Shi, and Y. Yan, *Appl. Phys. Lett.* **104**, 063903 (2014).
- [21] F. Brivio, A. B. Walker, and A. Walsh, *APL Mater.* **1**, 042111 (2013).
- [22] F. Brivio, K. T. Butler, A. Walsh, and M. van Schilfgaarde, *Phys. Rev. B* **89**, 155204 (2014).
- [23] S.-H. Wei and A. Zunger, *Appl. Phys. Lett.* **72**, 2011 (1998).
- [24] S. P. Kowalczyk, J. T. Cheung, E. A. Kraut, and R. W. Grant, *Phys. Rev. Lett.* **56**, 1605 (1986).
- [25] S. Chen, X. G. Gong, and S.-H. Wei, *Phys. Rev. B* **75**, 205209 (2007).
- [26] S. Chen, A. Walsh, J.-H. Yang, X. G. Gong, L. Sun, P.-X. Yang, J.-H. Chu, and S.-H. Wei, *Phys. Rev. B* **83**, 125201 (2011).
- [27] Q. Shu, J.-H. Yang, S. Chen, B. Huang, H. Xiang, X. G. Gong, and S.-H. Wei, *Phys. Rev. B* **87**, 115208 (2013).
- [28] Y.-H. Li, X. G. Gong, and S.-H. Wei, *Appl. Phys. Lett.* **88**, 042104 (2006).
- [29] Y.-H. Li, X. G. Gong, and S.-H. Wei, *Phys. Rev. B* **73**, 245206 (2006).
- [30] Y.-H. Li, A. Walsh, S. Chen, W.-J. Yin, J.-H. Yang, J. Li, J. L. F. DaSilva, X. G. Gong, and S.-H. Wei, *Appl. Phys. Lett.* **94**, 212109 (2009).
- [31] J. Junquera, M. H. Cohen, and K. M. Rabe, *J. Phys. Condens. Matter* **19**, 213203 (2007).
- [32] L. Colombo, R. Resta, and S. Baroni, *Phys. Rev. B* **44**, 5572 (1991).
- [33] A. Baldereschi, S. Baroni, and R. Resta, *Phys. Rev. Lett.* **61**, 734 (1988).
- [34] N. R. D’Amico, G. Cantele, and D. Ninno, *Appl. Phys. Lett.* **101**, 141606 (2012).
- [35] M.-G. Ju, G. Sun, J. Wang, Q. Meng, and W. Liang, *Appl. Mater. Interfaces* **6**, 12892 (2014).
- [36] G. Kresse and J. Furthmüller, *Comput. Mater. Sci.* **6**, 15 (1996).
- [37] J. P. Perdew, K. Burke, and M. Ernzerhof, *Phys. Rev. Lett.* **77**, 3865 (1996).
- [38] G. Kresse and D. Joubert, *Phys. Rev. B* **59**, 1758 (1999).
- [39] M. S. Hybertsen and S. G. Louie, *Phys. Rev. B* **34**, 5390 (1986).

- [40] J. T. Teherani, W. Chern, D. A. Antoniadis, J. L. Hoyt, L. Ruiz, C. D. Poweleit, and J. Menendez, *Phys. Rev. B* **85**, 205308 (2012).
- [41] M. L. W. Thewalt, D. A. Harrison, C. F. Reinhart, J. A. Wolk, and H. Lafontaine, *Phys. Rev. Lett.* **79**, 269 (1997).
- [42] R. Colombelli, V. Piazza, A. Badolato, M. Lazzarino, F. Beltram, W. Schoenfeld, and P. Petroff, *Appl. Phys. Lett.* **76**, 1146 (2000).
- [43] I. Vurgaftman, J. Meyer, and L. Ram-Mohan, *J. Appl. Phys.* **89**, 5815 (2001).
- [44] W. I. Wang, E. E. Mendez, and F. Stern, *Appl. Phys. Lett.* **45**, 639 (1984).
- [45] K. Heidrich, W. Schafer, M. Schreiber, J. Sochtig, G. Trendel, J. Treusch, T. Grandke, and H. J. Stolz, *Phys. Rev. B* **24**, 5642 (1981).
- [46] K. T. Butler, J. M. Frost, and A. Walsh, *Mater. Horiz.* **2**, 228 (2015).